JOURNAL OF MATERIALS SCIENCE **38** (2003) 1983–1994

The crystallization of calcium phosphate glass with the ratio $[CaO]/[P_2O_5] < 1$

M. B. TOSIĆ
Institute for the Technology of Nuclear and Other Mineral Raw Materials, Franchet d'Esperey 86, 11000 Belgrade, Yugoslavia
E-mail: m.tosic@itnms.ac.yu

R. Ž. DIMITRIJEVIĆ
Faculty of Mining and Geology, University of Belgrade, Djušina 7, 11000 Belgrade, Yugoslavia

M. M. MITROVIĆ
Faculty of Physics, University of Belgrade, Akademski trg 12-16, 11000 Belgrade, Yugoslavia

The phase evolution in a calcium phosphate glass with the molar ratio $[CaO]/[P_2O_5] < 1$, to which 6.4 mol% TiO_2 and 10 mol% Al_2O_3 were added as nucleation agents, was studied. The results indicate that the primary phase β-$Ca_2P_2O_7$ is formed during surface nucleation and crystallization which are dominant at $T < 930^\circ$C. No presence of metastable calcium phosphates was registered during the formation of the primary phase. The growth of β-$Ca_2P_2O_7$ crystals occurs on the faceted crystal/glass interface with dendritic morphology at a crystal growth rate that is independent of time. The kinetics of β-$Ca_2P_2O_7$ crystal growth are characterised by a growth activation energy of $E_a = 426 \pm 15$ kJ/mol. The parameters of the unit cell of the β-$Ca_2P_2O_7$ phase decrease with increasing temperature. The secondary TiP_2O_7 and $AlPO_4$ phases are formed by volume nucleation and crystallization. The temperature of the maximum nucleation rate was determined to be $T_n = 690^\circ$C, and it is higher than the transformation temperature T_g. In the temperature interval $T < 930^\circ$C secondary phases appear during long annealing times. At $T > 930^\circ$C glass volume crystallization is dominant.

1. Introduction

Studies of the crystallization behaviour of phosphate glasses till now have indicated their specificities regarding crystal nucleation and growth [1]. The reason for such behaviour may be found in their structure [2]. The basic structural elements of $[PO_4]$-tetrahedral phosphate glasses, as opposed to $[SiO_4]$ tetrahedral ones, have two types of network cation—oxygen bonds. Three bridging oxygens (BO) are connected by single bonds to the P-atom and via them the tetrahedron is connected to neighbouring $[PO_4]$-tetrahedra forming P—O—P bonds. The fourth oxygen atom is connected by a double bond to the P atom (P═O) (terminal oxygens-TO). Consequently, the behaviour of phosphate glasses differs in regard to the most widely used and studied silicate glasses. It is well known that phase separation in the glass is important in some cases for the controlled crystallization and formation of fine grained glass ceramics [3, 4]. It appears due to the different volume requirements of various molecular building units present in the glass, which tend to separate as distinct microphases [5]. Such behaviour appears in the case of phosphate invert glasses, which contain less than 50 mol% P_2O_5. Their structure consists of chains and isolated $[PO_4]$ units [6, 7]. However, a strong tendency toward phase separation is not expressed even in that case. Thus additional pathways must be sought for satisfying the criteria for the controlled crystallization of these glasses.

Reaney *et al.* [8] studied the crystallization of glasses from the CaO-P_2O_5 system with the ratio $[CaO]/[P_2O_5] \geq 1$ and showed the specific crystallization mechanisms of these glasses. Tošic *et al.* [9] studied the crystallization behaviour of glass powder from the system CaO-P_2O_5 with the molar ratio $[CaO]/[P_2O_5] < 1$, using the combination of Al_2O_3 and TiO_2 as nucleation agents. A complex crystallization behaviour depending on the powder particle size and crystallization temperature was shown. This paper is a continuation of the investigation of the crystallization of this glass whereby the nucleation and crystallization kinetics were studied. The investigations were performed under non-isothermal and isothermal crystallization conditions.

2. Experimental

Solid and liquid starting components were used to prepare the batches for melting. $CaCO_3$, $Al_2O_3 \cdot 3H_2O$ and TiO_2, reagent grade, and high purity quartz (99.9% SiO_2) were used as the solid components, while an aqueous solution of orthophosphoric acid (85 wt%

H_3PO_4) was used as the liquid component. The preparation of the mixture for melting has been described elsewhere [9]. The melting of the glass was performed in a Pt crucible in an electric furnace at $T = 1420°C$ for $t = 60$ min. The melt was cast on a steel plate and cooled in air. The solidified glass samples were transparent without residual bubbles.

The non-isothermal experiments were performed in a Netzch STA 409 EP device. Al_2O_3 powder was used as the reference material. The nucleation process was studied using powdered samples of 0.5–0.63 mm granulation. The samples were heated at the rate $v = 10°C$/min to the selected temperatures in the range 530–730°C at which they were held for $t = 180$ min and then further heated at the same rate to $T = 1100°C$. Experiments were performed with the following granulations: <0.038 and 0.5–0.63 mm at heating rates of 2, 5, 7, 10 and 12°C/min in order to evaluate the kinetic parameters of crystallization.

The second group of experiments was performed isothermally on bulk glass samples. The experiments were performed in an electric furnace with automatic temperature regulation (±1°C). The samples were isothermally treated in a two-step procedure. They were first annealed at a nucleation temperature of $T_n = 690°C$ for $t = 20$ h. Heating was then continued at a rate of $v = 2°C$/min to the selected crystallization temperature in the range $T_c = 770$–1100°C. The samples were kept at T_c for various times after which they were taken out of the furnace and crushed in an agate mortar. Favourable fractures were used for studying the crystal structure. The rest was milled and used for determination of the phase composition.

The X-ray diffraction (XRD) method was used to determine the phase composition. The X-ray powder diffraction patterns were obtained on a Philips PW-1710 automated diffractometer using a Cu tube operated at 40 kV and 32 mA. The instrument was equipped with a diffracted beam curved graphite monochromator and a Xe-filled proportional counter. The diffraction data were collected in the range of 4 to 70° 2θ Bragg angles counting 0.1 s (routine identification) and 2.5 s (calculation of unit/cell dimensions) at every 0.02° steps. The divergence and receiving slits were fixed 1 and 0.1, respectively. All the XRD measurements were performed at room temperature in a stationary sample holder. The LSUCRIPC program was used for the refinement of the cell dimensions from the powder data [10]. Cell dimension refinement was only utilised on the β-$Ca_2P_2O_7$ phase due to its early crystallization at lower temperatures. The refinement procedure was started using data for β-$Ca_2P_2O_7$ from the JCPDS card file (33-0297). After several cycles of successive indexing, with more and more reflections, most of the measured interplanar distances were indexed in the $P4_1$ space group [11, 12].

XRD data for β-$Ca_2P_2O_7$ broadening analysis were collected in the angular range between between 20 and 30, 2θ Bragg angles, covering only the (008) peak. This peak was scanned at every 0.02 steps counting 5 s per step. The alignment of the diffractometer was checked by means of a standard Si powder material whereas the instrumental resolution function was obtained from an annealed BaF_2 as the reference sample. The reason for the 008 peak broadening analysis was found in its relative purity. This peak is free of overlaps with other β-$Ca_2P_2O_7$ peaks, as well as TiP_2O_7 and $AlPO_4$ peaks appearing at temperature/time conditions of simultaneous crystallization. The measured (008) β-$Ca_2P_2O_7$ peak was modelled by the Pearson profile shape function using an interactive window program WinFit [13]. The crystallite size distribution was determined by integral breadth modelling using the single line analysis method.

The crystal morphology was investigated by scanning electron microscopy using a Jeol JSM 840 A microscope. The samples were gold sputtered in a Jeol JFC 1100 ionsputtering device.

TABLE I Glass composition

Glass composition	P_2O_5	CaO	Al_2O_3	TiO_2	SiO_2	$\frac{[CaO]}{[P_2O_5]}$
(mol%)	40.32	35.40	10.01	6.38	7.89	0.88
(wt%)	58.87	20.49	10.51	5.25	4.88	0.35

3. Results and discussion

3.1. The glass chemical composition

The results of the chemical analysis of the obtained glass are presented in Table I. It may be seen that a glass was obtained with the ratios $[CaO]/[P_2O_5] = 0.88$ and $[O]/[P] = 3.15$. Such a composition of phosphate glass has a structure consisting of phosphate chains which contain Q^1 and Q^2 tetrahedra [6, 7]. The SiO_2 present ensures glass formation, but does not influence its crystallization and remains amorphous during thermal treatment [8]. Al_2O_3 and TiO_2 were added as nucleating agents.

3.2. The nucleation behaviour

Fig. 1 shows the DTA curve of a sample of granulation <0.38 mm recorded at a heating rate $v = 10°C$/min.

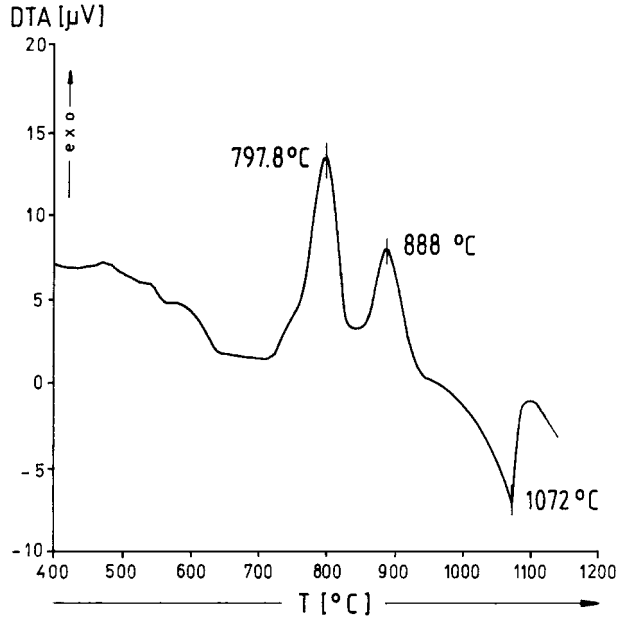

Figure 1 DTA trace recorded at a heating rate of 10°C/min for sample particle size <0.038 mm.

Two exothermal peaks were registered at a lower temperature (henceforth peak 1) $T_{p1} = 797.8°C$ and at a higher temperature (henceforth peak 2) $T_{p2} = 888°C$, as well as an endothermal peak at $T_1 = 1072°C$. The difference between the temperatures of peaks 1 and 2 is 90°C in the case of this sample. Investigations of the crystallization of this glass powder [9] have indicated that peak 1 appears in the temperature range $T < 900°C$ with increasing particle size up to 1 mm, at constant heating rate, while peak 2 appears in the range $T > 900°C$ and the temperature difference between the peaks increases up to 130°C. These investigations of the bulk samples have also shown that the β-$Ca_2P_2O_7$ phase is formed by the surface mechanism of crystallization at the temperatures of peak 1, while the TiP_2O_7 and $AlPO_4$ phases are formed by volume crystallization at the temperatures of peak 2. The endothermic peak is related to the melting onset of the β-$Ca_2P_2O_7$ phase. The results of SEM investigations of the bulk samples presented in this section and in section 3.3 also support this behaviour.

A method based on DTA measurements suggested by Marotta *et al.* [14] and Ray *et al.* [15] was used to investigate the nucleation behaviour. In order to apply this method the following conditions must be fulfilled: a) the crystal growth should occur on a constant number of nuclei during non-isothermal treatment and b) volume nucleation should take place in the glass. Dilatometric measurements of samples of this glass have indicated that its temperature of transformation is $T_g = 618°C$. The results of investigations of nucleation in glass up till now indicate that this process occurs at temperatures near the glass transformation temperature (T_g) [16]. Investigations of the crystallization of this glass powder have also shown that volume crystallization is dominant in the case of samples the particle size of which is >0.5 mm and at crystallization temperatures $T_c > 900°C$ [9]. These results suggest that the nucleation and crystal growth in this glass occur in temperature ranges, which are distinctly separate. By the appropriate choice of sample granulation and the heating rate in DTA experiments, it is possible to enable crystal growth at a constant number of nuclei. Consequently, a glass powder the dimensions of which were 0.5–0.63 mm and a heating rate of $\nu = 10°C/min$ were chosen for these experiments. Theoretical considerations [17, 18] have shown that the following relationship holds between the number of nuclei per unit volume and the temperature of the crystallization peak under non-isothermal conditions:

$$\ln(N) = \frac{E_a}{RT_p} + \ln \nu + \text{const}, \qquad (1)$$

where ν is the heating rate, T_p the temperature of the crystallization peak, E_a the activation energy of crystal growth and R the gas constant. Equation 1 enables the presentation of the correlation between $1/T_p$ and the nucleation temperature as a belltype curve similar to a nucleation curve. The maximum on this curve corresponds to the temperature of the maximum nucleation rate, T_n.

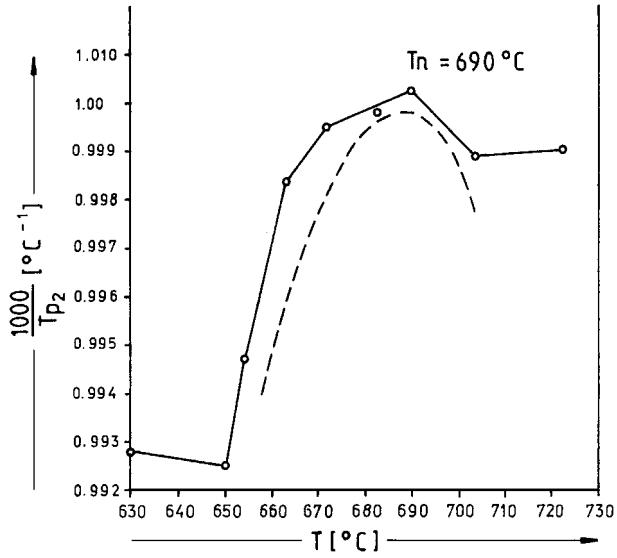

Figure 2 The dependence of $1/T_{p2}$ as a function of the nucleating temperature.

Previous analysis indicates that the nucleation behaviour of this glass may be analysed on the basis of the behaviour of T_{p2} at which volume crystallization of the selected sample occurs. The dependence of $1/T_{p2}$ on T was investigated in the temperature range $T = 530–730°C$. Fig. 2 shows the results for the temperature range $T = 630–730°C$ in which a curve with a maximum at $T = 690°C$ was detected. This temperature corresponds to the temperature of the maximum nucleation rate T_n. In that case the character of the nucleation process may be analysed from the ratio of T_n and T_g. When comparing T_n and T_g one may notice that T_n satisfies the condition that $T_n > T_g$ which indicates homogeneous glass nucleation [16].

Several additional experiments were performed in order to clarify the nucleation behaviour. Fig. 3 presents some of the XRD results recorded on samples crystallised at $T_c = 770°C$ for various times ranging from $t = 10–197$ h. The sample is amorphous after an

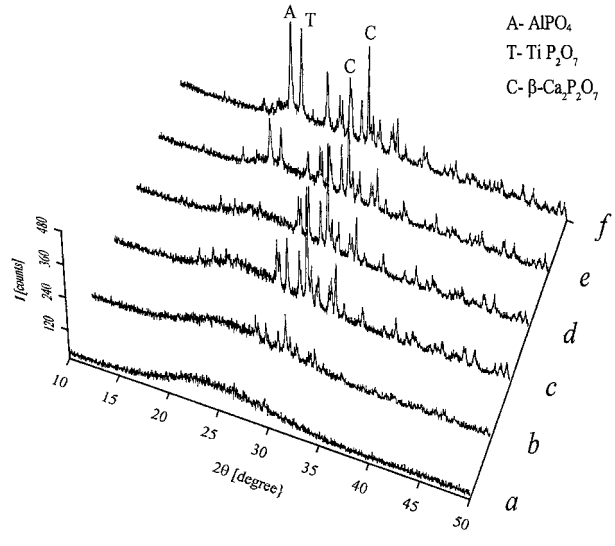

Figure 3 XRD patterns of bulk samples annealed at $T_c = 770°C$ for: a) $t = 10$ h, b) $t = 30$ h, c) $t = 80$ h, d) $t = 100$ h e) $t = 150$ h and f) $t = 197$ h.

annealing time of $t = 10$ h (Fig. 3a). At an annealing time of $t = 30$ h (Fig. 3b) the beginning of β-$Ca_2P_2O_7$ phase formation is registered. When the annealing time is increased to $t = 80$ h, only formation of the β-$Ca_2P_2O_7$ phase is registered. The formation of other $Ca_2P_2O_7$ polymorphs (α or γ) or of a metastable phase, as discussed by James *et al*. [1, 8], was not registered in that early stage of crystallization. At annealing times of $t = 80$ and 100 h (Fig. 3c and d) the presence of β-$Ca_2P_2O_7$ was also identified and the surface mechanism of crystallization is still dominant. Fig. 4a shows a SEM micrograph of a sample thermally treated at $T_c = 770°C$ for $t = 100$ h (XRD in Fig. 2d) which clearly shows crystallised layers on the external surfaces and the glass in the middle of the sample. The first traces of the formation of the TiP_2O_7 and $AlPO_4$ phases are noticed at the times $t = 80$ and 100 h (Fig. 3c and d). However, their presence is clearly identified at crystallization times of $t = 150$ and 197 h (Fig. 3e and f) when volume crystallization of the sample is dominant (Fig. 4b) and all three phases are present.

With increasing crystallization temperature T_c, SEM investigations of the samples treated at various temperatures indicate that the time during which surface crystallization is dominant sharply decreases to $T_c = 930°C$ at which surface crystallization is noticed only for very short times up to 15 min (Fig. 4c). At $T_c > 930°C$ volume crystallization is dominant (Fig. 4d) and XRD measurements indicate the presence of all three phases: β-$Ca_2P_2O_7$, TiP_2O_7 and $AlPO_4$.

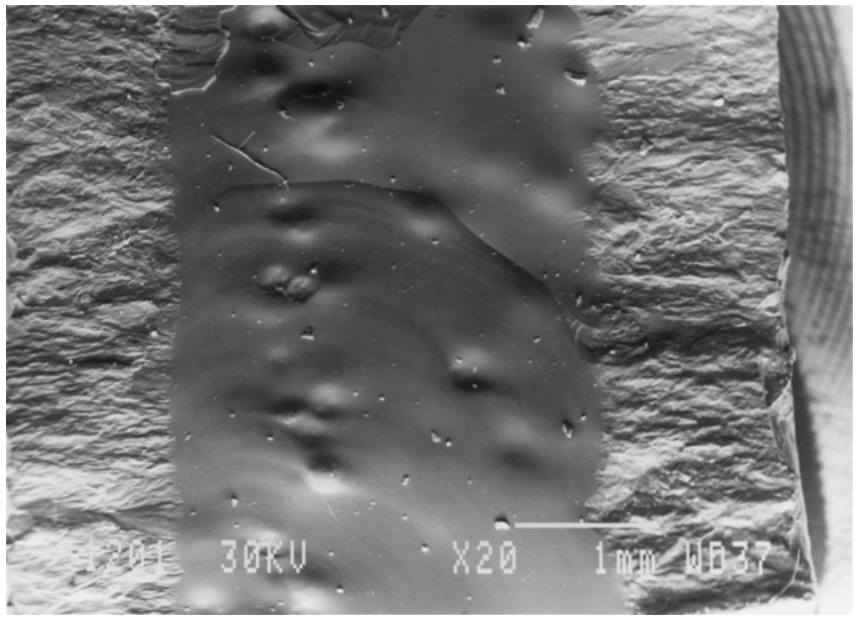

(a)

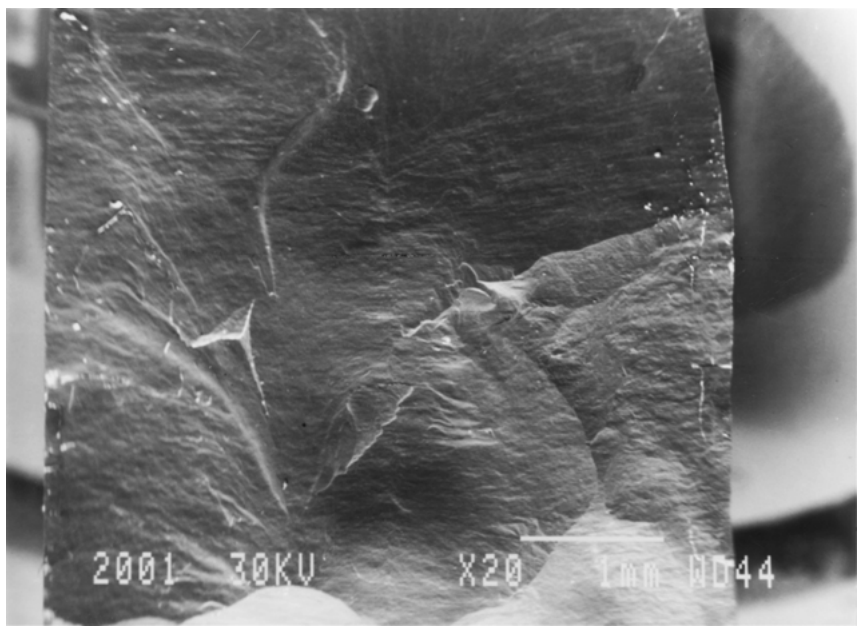

(b)

Figure 4 SEM micrograph of a sample with the following heat treatment: a) at $T_c = 770°C$ for $t = 100$ h, b) at $T_c = 770°C$ for $t = 150$ h, c) at $T_c = 930°C$ for $t = 15$ min and d) at $T_c = 960°C$ for $t = 15$ min. In all the experiments the samples were treated at $T_n = 690°C$ for $t = 10$ h before crystallization. (*Continued*)

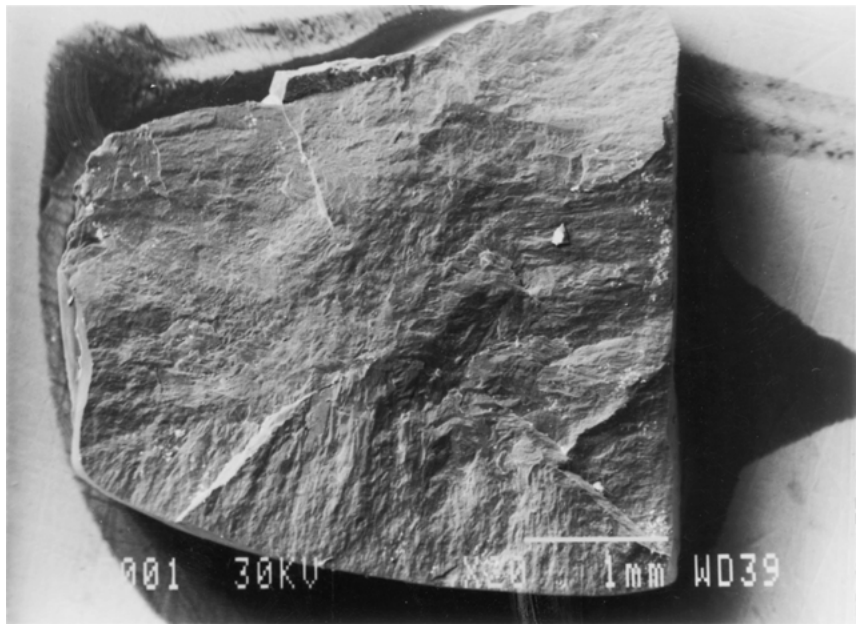

(c)

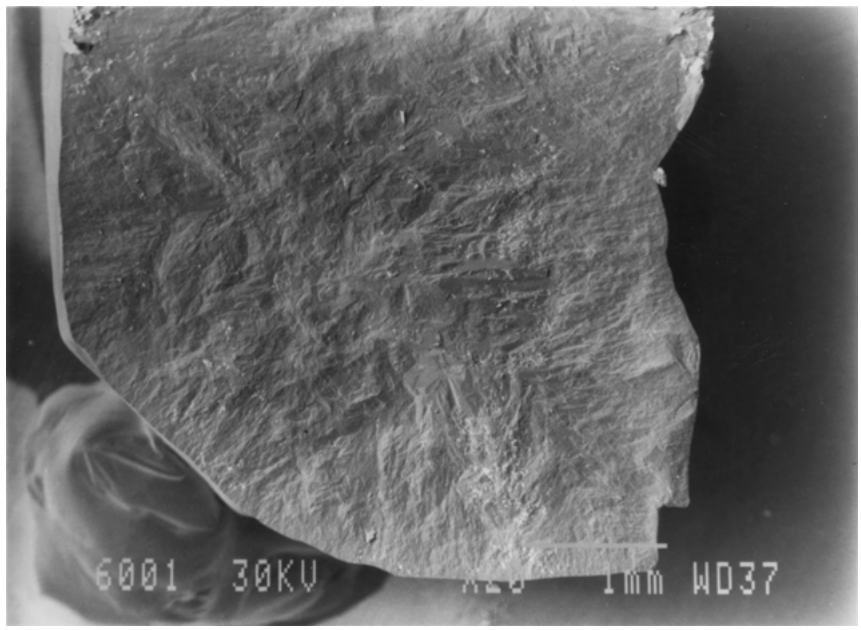

(d)

Figure 4 (*Continued*). $T_n = 690°C$ for $t = 10$ h, $T_n = 690°C$ for $t = 20$ h.

In all experiments the samples were thermally treated at $T_n = 690°C$ for $t_n = 20$ h in the first stage, so already formed nuclei were present during thermal treatment in the second stage at T_c. Fig. 5 shows the SEM micrographs of a sample thermally treated at $T_n = 690°C$ for $t_n = 20$ h in which drop-like regions indicating glass phase separation are registered. XRD measurements of this sample show that it is amorphous. Concurrently with the results of Reaney *et al*. [8] on the phase separation of calcium phosphate glasses of similar composition, these drop-like phases are rich in Ti, Al and P in which the nuclei of the TiP_2O_7 and $AlPO_4$ phases are formed in the subsequent stage. These results suggest that the presence of TiO_2 and Al_2O_3 in selected quantities in the case of this composition does not influence the nucleation of the primary β-$Ca_2P_2O_7$ phase because it is formed by the surface mechanism of crystallization in their presence. The presence of TiO_2 and Al_2O_3 in this case only enables volume nucleation of the secondary TiP_2O_7 and $AlPO_4$ phases. This is then followed by the volume crystallization of the glass, indicating homogeneous nucleation, which is also indicated by the found ratio that $T_n > T_g$.

3.3. Crystallization kinetics

3.3.1. Treatments under isothermal conditions

Formation of the primary β-$Ca_2P_2O_7$ phase by the surface mechanism of crystallization at lower temperatures, without the appearance of secondary phases, enables analysis of the crystal growth rate of this phase under isothermal experimental conditions. Thus, three different groups of experiments were performed using

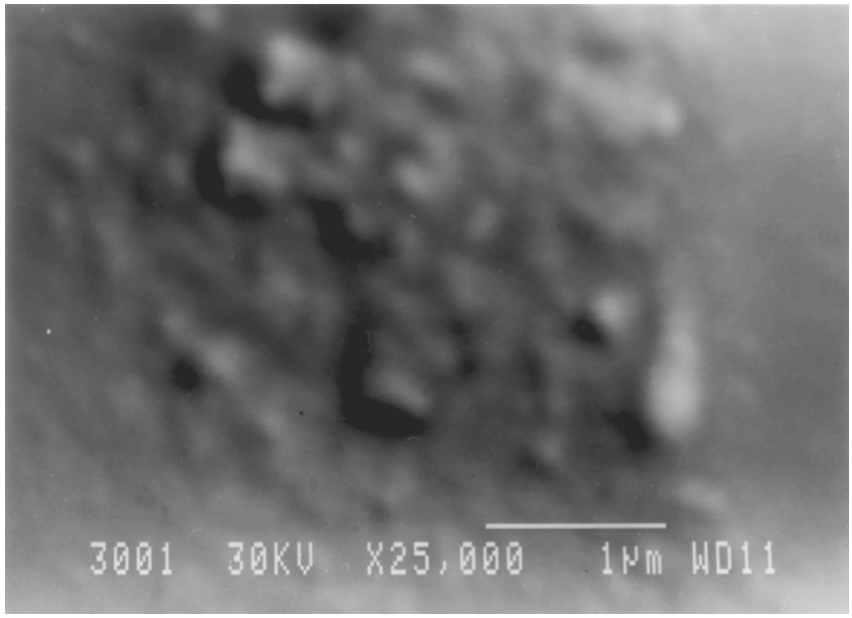

Figure 5 SEM micrograph of a sample with the following heat treatment: $T_n = 690°C$ for $t_n = 20$ h.

bulk samples. The first group of experiments was performed at $T_c = 770°C$, which is near the lowest temperature of crystallization peak 1 in the DTA curve recorded on a sample of <0.038 mm granulation at the heating rate $\nu = 2°C/min$ (Table II). Some of the XRD results of these experiments are presented in Fig. 3. It is obvious from this figure that the crystallization of the primary β-$Ca_2P_2O_7$ phase may easily be followed by the successive increase of the intensity of the characteristic reflection with the Miller index (008) at the Bragg angle $2\theta = 29.60°$. This reflection is not influenced by other reflections of the tetragonal crystalline lattice, which enables reliable measurement of the change of the width of the peak intensity and calculation of the microstructural parameters. Also in the case when all three phases are present in the diffractogram, the (008) peak of β-$Ca_2P_2O_7$ is still unaffected by the reflections of the other two phases. The dimension of the β-$Ca_2P_2O_7$ crystallite was calculated along the c axis in each experiment using the WinFit program [13].

Fig. 6 shows the change in the crystallite dimension $\langle D \rangle$ along the axis c with time at the crystallization temperature $T_c = 770°C$. It may be seen from the figure that the parameter $\langle D \rangle$ linearly increases with time up to $t = 150$ h. As previously shown in Section 3.2, for times $t < 150$ h the surface crystallization of β-$Ca_2P_2O_7$ dominates at this temperature. The total crystallite density is low and the crystallite dimension increase may be followed as a function of time. Such an increase of the crystallite dimension indicates that the rate of β-$Ca_2P_2O_7$ crystal growth is independent of time, i.e. a steady-state growth rate is rapidly attained. At annealing times $t > 150$ h the parameter $\langle D \rangle$ decreases. There are many reasons for such behaviour of parameter $\langle D \rangle$. Volume crystallization of the sample dominates at long annealing times and the presence of the new TiP_2O_7 and $AlPO_4$ phases is identified. The total density of the present crystallites in the sample increases and β-$Ca_2P_2O_7$ crystallites quickly come into contact with neighbouring crystallites so their dimensions remain limited, i.e. the growth rate becomes zero. Besides, due to the increase in crystallite density, the fraction of crystalline phases sharply increases as does the strain in the sample causing microfractures of the already formed β-$Ca_2P_2O_7$ crystallites thus also decreasing the crystallite dimensions at times $t > 150$ h.

TABLE II Shift of the peaks as a function of the heating rate for powdered glass particle sizes <0.038 and 0.5–0.63 mm

Heating rate (°C/min)	Particle size <0.038 mm		Particle size 0.5–0.63 mm	
	T_{p1}(°C)	T_{p2}(°C)	T_{p1}(°C)	T_{p2}(°C)
2	763	844	830	923
5	783.2	867.8	852.2	960.4
7	788.1	879	860.8	980.7
10	797.8	888	868	998.8
12	800.4	889.2	875.8	1007.6

Experiments using bulk samples thermally treated for $t = 80$ h at various temperatures in the interval $T = 770$–$1100°C$ were performed in order to study the influence of temperature on β-$Ca_2P_2O_7$ crystallite dimensions along the c axis. Fig. 7 shows the changes of crystallite dimension $\langle D \rangle$ along the c axis as a function of temperature. It may be seen from Fig. 7 that in the temperature range $T < 930°C$, in which surface crystallization dominates, parameter $\langle D \rangle$ increases, while it decreases with increasing temperature in the temperature range $T > 930°C$ where volume crystallization is dominant. Comparison of the results for these two groups of experiments clearly shows that the changes in β-$Ca_2P_2O_7$ crystallite dimensions with time and temperature are similar and caused by a change in the glass crystallization mechanism.

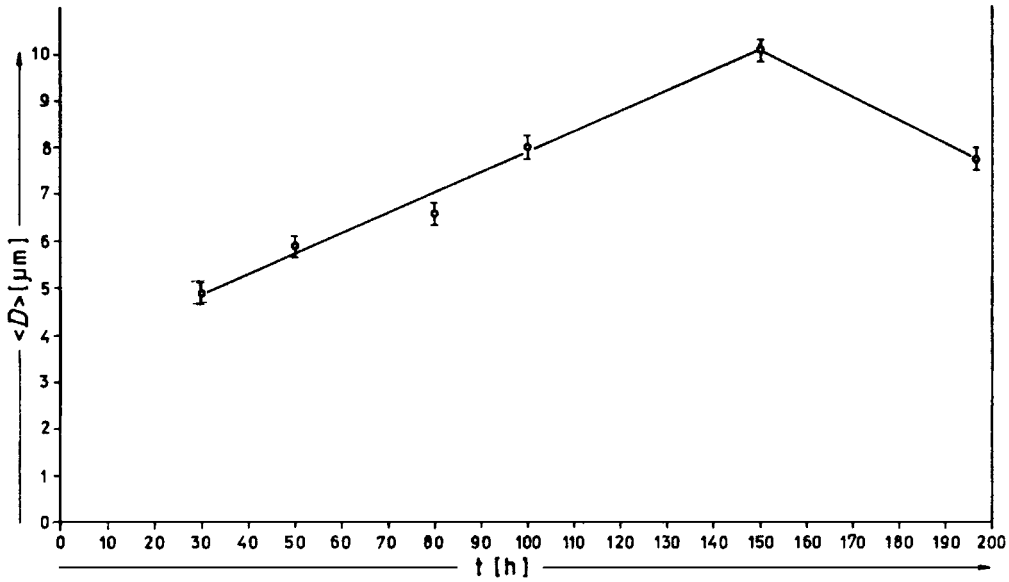

Figure 6 Changes in the β-$Ca_2P_2O_7$ crystallite dimension along the c axis $\langle D \rangle$ as a function of time at $T_c = 770°C$.

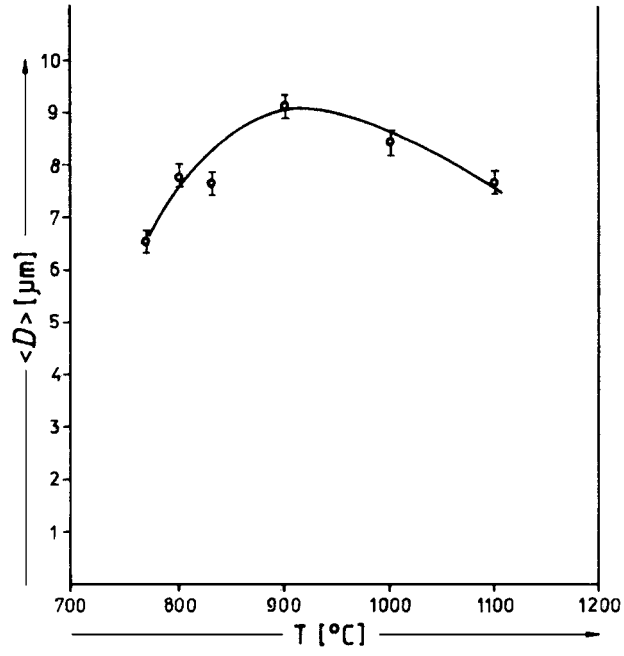

Figure 7 Changes in the β-$Ca_2P_2O_7$ crystallite dimension along the c axis $\langle D \rangle$, formed during an annealing time of $t = 80$ h, at various crystallization temperatures in the interval $T = 770$–$1100°C$.

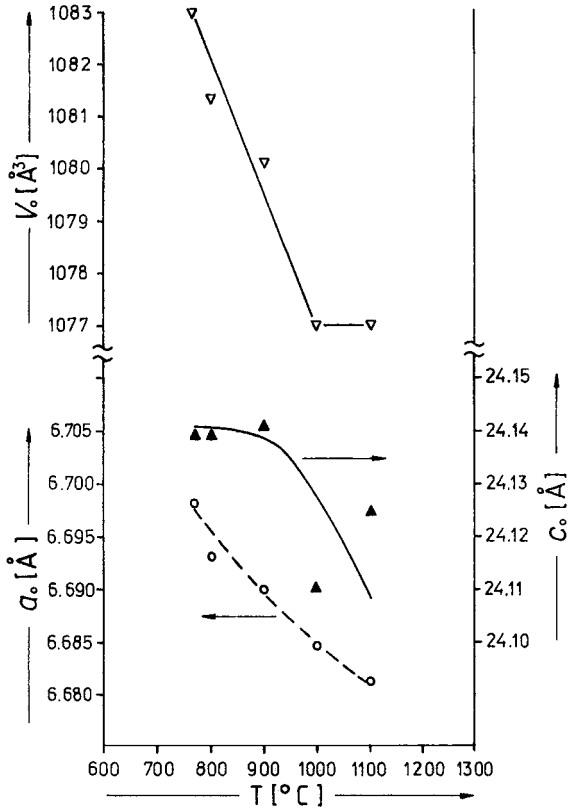

Figure 8 Changes in the unit cell parameters (a_o, c_o and V_o) of the β-$Ca_2P_2O_7$ phase as a function of temperature.

The parameters of the unit cell (a_o, c_o and V_o) of the β-$Ca_2P_2O_7$ phase of each sample were also calculated using the results of this group of experiments and the LSUCRIPC program [10]. Fig. 8 shows the changes of these parameters as a function of temperature. It may easily be seen from Fig. 8 that these parameters generally decrease with increasing temperature. This change is almost linear along the crystallographic axis a. However, along the c axis somewhat different behaviour may be noticed. In the temperature range $T < 900°C$ the parameter c_o is practically constant and then at $T > 900°C$ there is a sudden drop. Parameter V_o clearly shows a decrease with increasing temperature up to $T = 1000°C$. Above this temperature the unit cell does not change. Such behaviour of the unit cell parameters of β-$Ca_2P_2O_7$ is related to structural changes in this phase in early stages of the crystallization and indicates the complexity of this process in the investigated composition.

In the authors' opinion there are two reasons why these changes occur. The first regards the phenomenon of isomorphism. In the early stages of β-$Ca_2P_2O_7$ phase formation some of the network (P^{5+}) or non-network (Ca^{2+}) cations may be replaced by other present cations (Ti^{4+} or Al^{3+}) from the glass composition which, according to Vegard's rule, influences the increase of the unit cell dimensions of the β-$Ca_2P_2O_7$ phase. During further thermal treatment their substitution is

performed by diffusion, which leads to changes in the β-$Ca_2P_2O_7$ unit cell dimensions. The Ca^{2+} cation is well known for its isomorphism and variable coordination, which ranges from 6 to 9, which is often the case especially in silicates and zeolites [19]. Also, the P^{5+} cation may be replaced by cations with a larger ionic radius Al^{3+} and Ti^{4+}, which build tetrahedral networks (aluminates and titanates). In this composition they are unstable, which during thermal treatment leads to substitution by the P^{5+} cation and their expulsion from the phosphate network.

The second reason for changes in the β-$Ca_2P_2O_7$ unit cell dimensions may be "hidden" polymorphism. The composition $2CaO \cdot P_2O_5$ is known for its larger number of crystalline polymorphic modifications: α-phase (JCPDS 45-1061), β-phase (JCPDS 33-0297), 7.38 A phase (JCPDS 410489),γ-phase (JCPDS 23-0871) and UN-phase (James *et al.* [1, 8, 20]). During these experiments the presence of no other polymorph beside β-$Ca_2P_2O_7$ was detected. However, it is still possible that there was simultaneous formation of the UN-phase and β-$Ca_2P_2O_7$. Due to the great similarity of the XRD, the UN phase may be "masked" by the diffraction maxima of the β-$Ca_2P_2O_7$ phase. If one assumes that the unit cell dimensions of the UN phase (which was not calculated and about which there are very few data) are somewhat larger than those of β-$Ca_2P_2O_7$, which is also implied by the available XRD data [8, 20], then the changes in Fig. 8 could represent the transformation from the UN to the β-$Ca_2P_2O_7$ phase. The assumption about the existence of an early stage of crystallization, a so-called Low β-$Ca_2P_2O_7$ polymorph which is unstable and which with increasing temperature transforms to the High β-$Ca_2P_2O_7$ phase, is also interesting in this situation. Due to the non-stoichiometric composition of the glass and the probable displasive character (without the scission of chemical bonds) and with mild symmetry changes and shifts in interatomic distances, this transformation is "hidden" and is manifested by the changes displayed in Fig. 8.

The third group of experiments was performed using bulk samples thermally treated for various times at crystallization temperatures in the range $T = 770$–930°C in order to determine the influence of temperature on the β-$Ca_2P_2O_7$ crystal growth rate. Appropriate sample fractures were used for SEM investigations in which the thickness of the surface crystallised layer of β-$Ca_2P_2O_7$ was measured, structure of the crystal/glass interface studied, as was the crystal growth morphology. Fig. 9a and b show SEM micrographs of samples thermally heated at $T_c = 860^\circ$C for $t = 0.5$ h. It may be seen from these micrographs that the β-$Ca_2P_2O_7$ crystals grow on the facet boundaries with dendritic morphology.

The molar entropy of fusion of $Ca_2P_2O_7$ crystals is $\Delta S_m = 62,015$ J/mol K [21]. In this case, according to the Jackson criterion, $\Delta S_m > 4R$ and the most closely packed interface planes should be smooth on an atomic scale [22]. If the interface is atomically smooth, growth with faceted interface morphology occurs and the growth rate is highly anisotropic and determined by crystal defects. When the melt and crystal have the same chemical composition, for the case of growth at step sites provided by a screw dislocation intersecting the interface, the growth rate may be expressed by the relation [23]

$$u = K(\Delta T)^{2(1-\varepsilon)} \exp(-E_a/RT) \qquad (2)$$

where $0 < \varepsilon < 1$ and the parameters ε, K and E_a are considered to be independent of T, $\Delta T = T_l - T$ where T_l is the liquidus temperature. Equation 2 provides the basis for the presentation of the growth rate data. Fig. 10 shows the observed growth rates of the crystallised β-$Ca_2P_2O_7$ layer in the temperature range $T = 770$–930°C. If the liquidus temperature is taken to be the endothermal peak on the DTA curve $T_l = 1072^\circ$C, the observed growth rates of the crystalline layer may be fitted by the least squares method by Equation 2. The largest correlation coefficient of 0.997 was obtained in the interval $\varepsilon = \{0; 0.15\}$. The mean value $\varepsilon = 0.075$ was chosen for further calculations. The following equation is obtained by introducing this value to Equation 2:

$$\ln[u/(\Delta T)^{1.85}] = \ln K - E_a/RT \qquad (3)$$

Fig. 11 shows the relationship of the left side of Equation 3 with $1/T$. It may be seen from Fig. 11 that the observed growth rates of the crystalline layer fit this equation well. The values of the parameters K and E_a in Equation 3 are: $K = 1.04 \cdot 10^{16}$ μm/s and $E_a = 452 \pm 17$ kJ/mol.

As the compositions of the glass and crystal of β-$Ca_2P_2O_7$ are different, the crystal growth kinetics may be limited by interdiffusion into the glass (diffusion-controlled growth) and phase boundary reactions on crystal/glass (interface-controlled growth), which is designated as mixed control. Analysing the crystal growth kinetics for this case Qian *et al.* [23] obtained the following relationship:

$$u = \frac{K_1 K_2}{(\sqrt{K_2} + 1)^2} \left(\frac{\Delta T}{T_m}\right)^2 \exp[-(E_a/RT)] \qquad (4)$$

where K_1 is a parameter independent of temperature, K_2 a parameter dependent on temperature and T_m the melting temperature. Equation 4 is similar in form to Equation 2 for $\varepsilon = 0$. However, they differ in the fact that the ratio $K_1K_2/(K_2^{1/2} + 1)^2$ may depend on temperature, while K in Equation 2 is considered to be independent of temperature. If $K_2 \gg 1$ the growth kinetics are defined by the phase boundary reaction. On the other hand, when $K_2 \ll 1$ the kinetics are defined by diffusion-controlled growth in the glass. Solutions for K_2 are obtained from Equations 3 and 4:

$$K_{2(1,2)} = \frac{(K^2C^2 + KCK_1) \pm \sqrt{(K^2C^2 + KCK_1)^2 - 4K^2C^2(K_1 - KC)^2}}{2(K_1 - KC)^2} \qquad (5)$$

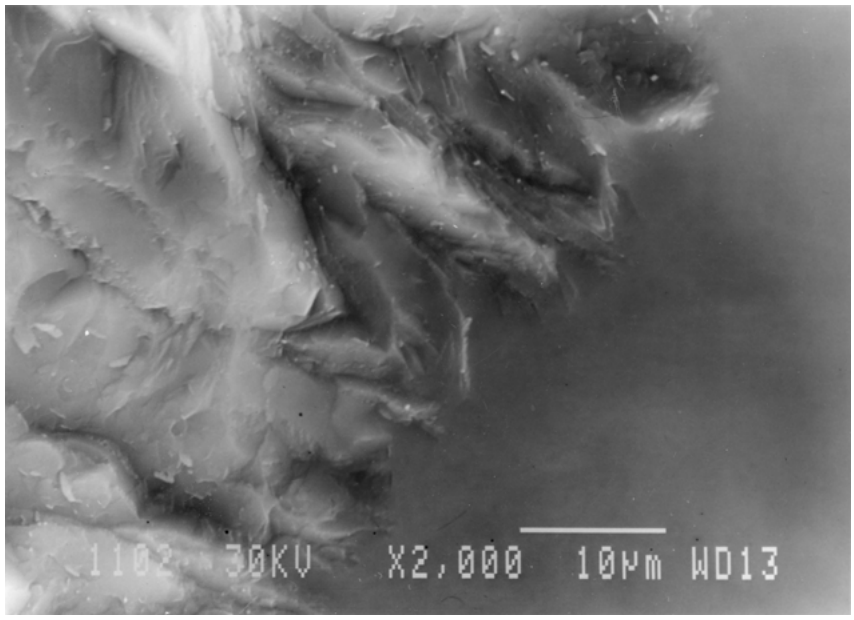

(a)

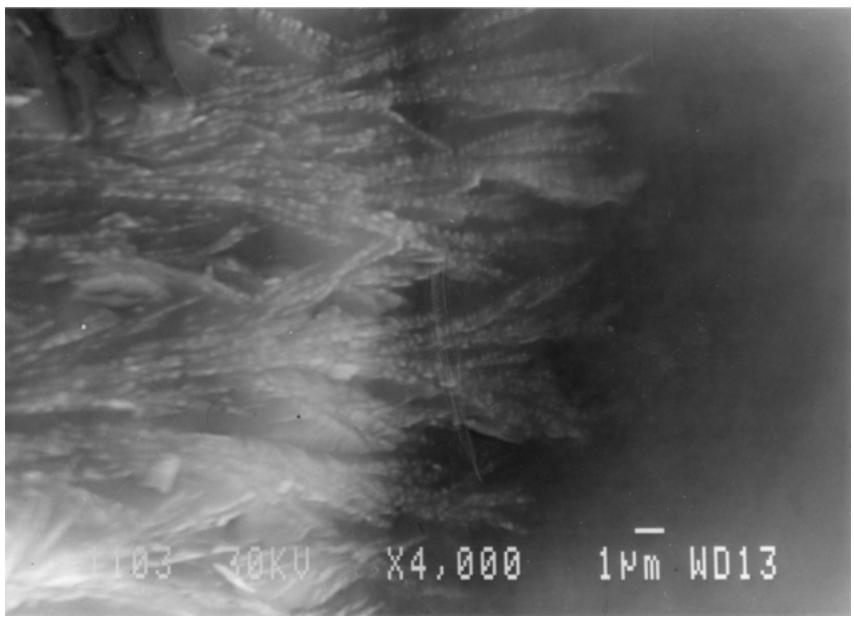

(b)

Figure 9 SEM micrographs of a sample with the following heat treatment: $T_n = 690°C$ for $t_n = 20$ h and $T_c = 860°C$ for $t = 0.5$ h: a) interface crystal/glass and b) dendritic structure of β-$Ca_2P_2O_7$.

where $C = T_m^2/(\Delta T)^{0.075}$. For the solutions for K_2 to be real it is necessary to fulfil the condition $K > K_1 T_m^{2/3}(\Delta T)^{0.075}$. Parameter $K_1 = \Delta H_m^2/12\pi^2 \sigma V \eta_o \lambda$, where ΔH_m is the melting enthalpy per molecule at $T = T_m$, V-the molecular volume of the crystal, σ-the crystal-melt interfacial energy, λ-the jump distance and η_o-the pre-exponential factor. The value of parameter K_1 was calculated on the basis of available data to be $K_1 = 4.29 \times 10^{-14}$ m/s. Using the calculated values for K and K_1 in Equation 5, real solutions were obtained for the parameter K_2 of the order of magnitude $K_2 \approx 10^4$ which indicates that $K_2 \gg 1$. That suggests that the β-$Ca_2P_2O_7$ crystal growth kinetics is, in this case, interface-controlled. When $K_2 > 1$ dendritic growth sufficiently accelerates the diffusion process so that boundary phase reactions have a greater influence on the growth kinetics. On the basis of this analysis and the of SEM investigations, which have shown that β-$Ca_2P_2O_7$ crystals grow with a faceted interface (Fig. 9a), it may be concluded that β-$Ca_2P_2O_7$ crystals grow according to the model of screw dislocation growth.

3.3.2. Treatments under non-isothermal conditions

As the temperature intervals of nucleation and crystal growth are distinctly separate in this case, it is possible for crystallization to proceed with a constant number of nuclei by selecting low heating rates during non-isothermal treatment. In this way the complicated temperature dependence of the nucleation rate is avoided

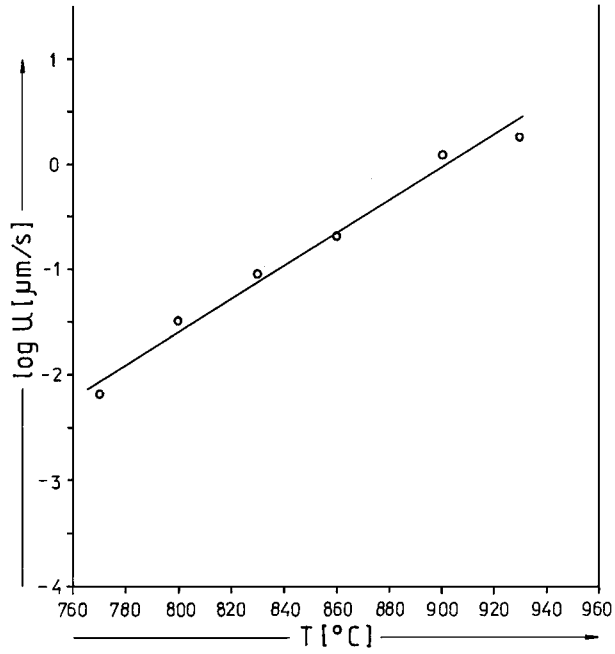

Figure 10 Growth rate of the crystallized layer of β-$Ca_2P_2O_7$ as a function of temperature in the temperature range T = 770–930°C.

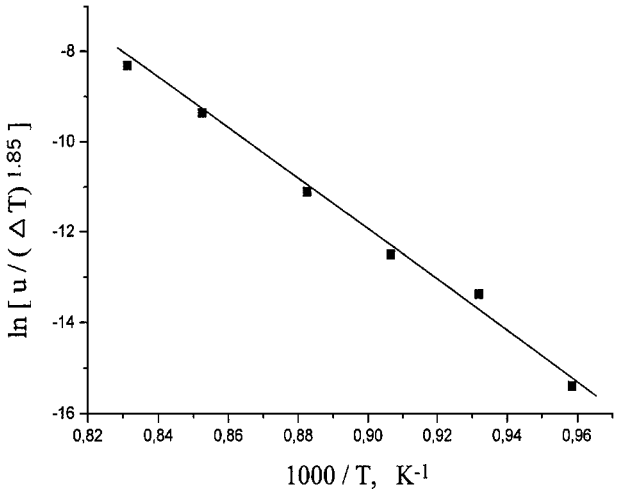

Figure 11 The plot of $\ln[u/(\Delta T)^{1.85}]$ versus $1/T$.

and the problem reduces to the temperature dependence of the crystal growth rate. The experimental results in Section 3.3.1 suggest that the kinetics of dendritic growth of β-$Ca_2P_2O_7$ is interface-controlled in the temperature interval T = 770–930°C. However, the rate-controlling mechanism of the crystal growth rate may differ at various temperatures [23]. When $T > T_m$, K_2 in Equation 4 becomes much larger than one ($K_2 \gg 1$) which corresponds to interface-controlled growth. Consequently, it is reasonable to assume in the case of this glass that even at temperatures $T > 930$°C that the same rate-controlling mechanism of β-$Ca_2P_2O_7$ crystal growth is operational. In that case the Kissinger method may be applied for the analysis of the non-isothermal experimental data for the crystallization of the primary β-$Ca_2P_2O_7$ phase. The modified form of the Kissinger equation [24] is:

$$\ln\left(\frac{\nu^n}{T_p}\right) = -\frac{mE_a}{RT_p} + \text{const.} \qquad (6)$$

where n is the Avrami exponent and m denotes the dimensionality of crystal growth. The values of parameters n and m depend on the rate controlling mechanism of crystallization kinetics, while the value of E_a is obtained from the ratio $\ln(\nu^n/T_p^2)$ vs. $1/T_p$ by using the corresponding values for n and m. In cases when the experiments were performed in such a way that the glass samples were saturated with nuclei before crystal growth, then parameter E_a may be interpreted as the activation energy of crystal growth [25, 26].

Two powdered samples of the granulations <0.038 mm and 0.5–0.63 mm were chosen for the non-isothermal experiments and heated at different heating rates ranging from 2 to 12°C/min. The T_p temperatures recorded for both specimens at different heating rates are presented in Table II. The surface crystallization mechanism of β-$Ca_2P_2O_7$ formation dominates in the case of the glass powder with larger particle sizes of 0.5–0.63 mm, based on the values of the DTA peak 1 [9]. As the crystal growth in these DTA experiments takes place on a constant number of nuclei, then in this case $n = m = 1$ and Equation 6 is equal to the well known Kissinger equation. An activation energy of β-$Ca_2P_2O_7$ crystal growth of $E_{a1} = 403 \pm 15$ kJ/mol (line A_1, Fig. 12) was calculated for peak 1 by applying the Kissinger equation. At the temperatures of peak 2, volume crystallization dominates during which the secondary TiP_2O_7 and $AlPO_4$ phases are formed [9]. The results in Sections 3.2 and 3.3 indicate that the $AlPO_4$ phase appears last which indicates that its formation controls the total crystallization process of this glass under these conditions, so the calculated value of E_{a2} may be ascribed to the crystal growth of $AlPO_4$. As the crystal growth occurs on a constant number of nuclei then $n = m$ so Equation 6 is again equal to the Kissinger equation. An activation energy of crystal growth of $E_{a2} = 245 \pm 7$ kJ/mol was determined by applying the Kissinger method to peak 2 (line A_2, Fig. 12).

The values of parameter n may be determined on the basis of the same DTA curves. The value of parameter n indicates the mechanism of crystal growth. Parameter n was determined according to the Ozawa method [27] from the following equation:

$$\left.\frac{d(\log[-\ln(1-x)])}{d\log\nu}\right|_T = -n \qquad (7)$$

where x is the volume fraction crystallised in time t. This method avoids the assumption of the temperature dependence of the rate coefficient. It thus enables a reasonable estimation of parameter n [26]. The values of x are obtained from the ratio $x = S/S_o$ where S designates the peak surface at the chosen temperature, while S_o is the total surface of the corresponding peak. The positions of the crystallization peaks at various heating rates on the DTA curves of this sample enable the determination of three values of x at the chosen temperature. DTA curves recorded at heating rates of ν = 5, 7 and 10°C/min were used for these calculations. The temperature T = 860.8°C was selected for calculations on peak 1 and T = 960.4°C for peak 2. The values of n on

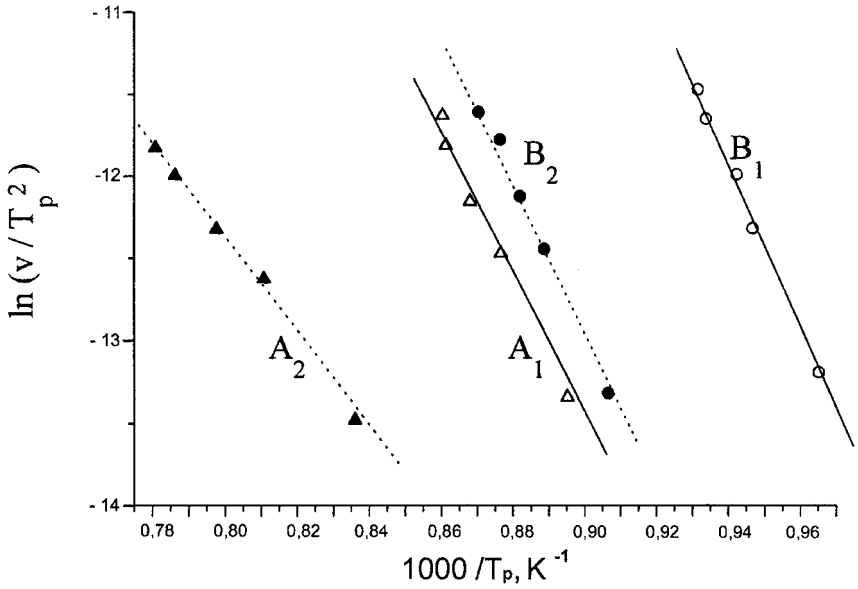

Figure 12 The plot of $\ln(\nu/T_p)$ versus $1/T$ for the powder sample particle sizes: A_1) 0.5–0.63 mm, peak 1, $n = m = 1$ and A_2) 0.5–0.63 mm, peak 2, $n = m = 1$, B_1) <0.038 mm, peak 1, $n = 1$, B_2) <0.038 mm, peak 2, $n = 1$.

peak 1, $n_1 = 1.25 \pm 0.2$ and on peak 2, $n_2 = 3.23 \pm 0.4$ were obtained by using Equation 7. In the case of this sample surface crystallization is dominant at the temperatures of peak 1, while the volume mechanism is dominant at the temperatures of peak 2. Therefore, for interface-controlled crystal growth, at a constant number of nuclei, theoretical values of parameter n [28] are operational: for peak 1, $n_1 = 1$ and for peak 2, $n_2 = 3$. By comparing the values of parameter n and taking into consideration experimental error, one may conclude that there is good agreement between the experimentally determined and theoretical values. This also confirms that the previous analyses in Section 3.3.1 on the kinetics of β-$Ca_2P_2O_7$ crystal growth by interface-controlled growth were correct.

In the case of the sample with granulation <0.038 mm the particle sizes are the smallest. It was also shown that at these particle sizes both crystallization peaks have dominant surface crystallization [9]. It may, therefore, be considered that in this case the condition of the constant number of nuclei in the DTA experiments was secured. On the basis of the recorded T_p's at various heating rates, presented in Table II, and by using the value of the parameter $n = 1$ for both peaks, the values of the activation energy E_a were calculated according to Equation 6: on peak 1 $E_{ap1} = 421 \pm 16$ kJ/mol (line B_1, Fig. 12) and on peak 2 $E_{ap2} = 389 \pm 21$ kJ/mol (line B_2, Fig. 12). The XRD results also showed that in this case at the temperatures of peak 1 only β-$Ca_2P_2O_7$ is formed by the surface crystallization mechanism, while all three phases β-$Ca_2P_2O_7$, TiP_2O_7 and $AlPO_4$ are identified at the temperatures of peak 2 [9]. Consequently, the calculated values of E_a on peak 1 for both samples of granulation <0.038 and 0.5–0.63 mm may be compared, as well as with the value of the same parameter calculated on bulk samples in isothermal experiments, Section 3.3.1, because they regard the formation of only the β-$Ca_2P_2O_7$ phase by the surface crystallization mechanism. By comparing the obtained values of E_a, it may easily be noticed that there is good agreement within experimental error, so the mean value of $E_a = 426 \pm 15$ kJ/mol was adopted for the formation of the primary β-$Ca_2P_2O_7$ phase. However, in the case of the sample with the granulation <0.038 mm at the temperatures of peak 2, the surface crystallization mechanism is dominant and the presence of all three phases was identified. As the relationship between the rate of formation of these three phases by the surface crystallization mechanism is not quite clear, it is unclear what the calculated value of the parameter $E_{ap2} = 389 \pm 21$ kJ/mol refers to. Therefore, this value should not be compared to the value $E_{a2} = 245 \pm 7$ kJ/mol determined at the temperatures of peak 2 in the case of the sample with the granulation 0.5–0.63 mm.

4. Conclusions

The subject of these investigations was the nucleation and crystallization kinetics of calcium phosphate glass with the molar ratio $[CaO]/[P_2O_5] < 1$ and the nucleating agents 6.4 mol% TiO_2 and 10 mol% Al_2O_3. The volume nucleation of this glass occurs in the temperature range above the transformation temperature T_g and the temperature of the maximum nucleation rate is at $T_n = 690°C$. Nucleation is preceded by phase separation of the glass. The nuclei of the secondary TiP_2O_7 and $AlPO_4$ phases are formed during volume nucleation. The results indicate that the nucleating agents TiO_2 and Al_2O_3 did not stimulate the nucleation of the primary β-$Ca_2P_2O_7$ phase at this composition. Crystal growth occurs in the temperature range $T = 770$–$1100°C$ in the following way:

At $T < 930°C$ surface crystallization of the primary β-$Ca_2P_2O_7$ phase is dominant. The crystal growth of this phase takes place on the faceted crystal/melt boundaries with dendritic morphology. The rate of crystal growth is independent of time. The influence of temperature on the growth rate is characterised by an activation energy of $E_{al} = 426 \pm 15$ kJ/mol. The crystal growth

kinetics is controlled by phase boundary reactions. The formation of metastable of $Ca_2P_2O_7$ in the early stages of crystallization was not registered. The parameters of the unit cell of $Ca_2P_2O_7$ decrease with increasing temperature. The secondary TiP_2O_7 and $AlPO_4$ phases are formed at long times which leads to a change in the crystallization mechanism from surface to volume glass crystallization. Consequently, there is a large increase in the total crystallite density, increased strain and a decrease in the crystallite dimensions of the primary β-$Ca_2P_2O_7$ phase. With increasing temperature the time at which the glass crystallization mechanism changes suddenly decreases.

At $T > 930^{\circ}C$ volume crystallization is dominant and the TiP_2O_7 and $AlPO_4$ secondary phases are formed. The crystallite dimensions and parameters of the unit cell of the primary β-$Ca_2P_2O_7$ phase also decrease with increasing temperature in this temperature range. The total glass crystallization kinetics are determined by the formation of the $AlPO_4$ phase with a crystal grwoth activation energy of $E_{a2} = 245 \pm 7$ kJ/mol.

Acknowledgment

The authors acknowledge the financial support from the Serbian Ministry of Science, Technology and Development (Grants No.: 1818, MHT. 2. 07. 0026. B and 1578).

References

1. P. F. JAMES, Y. IQBAL, U. S. JAIS, S. JORDERY and W. E. LEE, *J. Non-Cryst. Solids* **219** (1997) 17.
2. W. VOGEL and W. HÖLAND, *Angw.: Chem. Int. Ed. Engl.* **26** (1987) 527.
3. M. B. TOŠIČ, M. M. MITROVIĆ and R. Ž. DIMITRIJEVIC, *J. Mater. Sci.* **35** (2000) 3659.
4. M. B. TOŠIĆ, R. Ž. DIMITRIJEVIĆ and M. M. MITROVIĆ, *ibid.* **37** (2002) 2293.
5. P. F. JAMES, *ibid.* **10** (1975) 1802.
6. R. K. BROW, *J. Non-Cryst. Solids* **263/264** (2000) 1.
7. U. HOPPE, *ibid.* **195** (1996) 138.
8. I. M. REANEY, P. F. JAMES and W. E. LEE, *J. Amer. Ceram. Soc.* **79** (1996) 1934.
9. M. B. TOŠIĆ, M. M. MITROVIĆ, R. Ž. DIMITRIJEVIĆ and N. S. BLAGOJEVIĆ, *J. Mater. Sci.* **37** (2002) 4369.
10. R. GARNEY, *Powd. Diff.* **1** (1986) 114.
11. N. C. WEBB, *Acta Cryst.* **21** (1966) 942.
12. S. BOUDIN, *ibid.* C **49** (1993) 2062.
13. S. KRUMM, *Mater. Sci. Forum* **228–231** (1996) 183.
14. A. MAROTTA, A. BURII and F. BRANDA, *J. Mater. Sci.* **16** (1981) 341.
15. C. S. RAY and D. E. DAY, *J. Amer. Ceram. Soc.* **73** (1990) 439.
16. E. D. ZANOTTO and M. C. WEINBERG, *Physics Chem. Glasses* **19** (1989) 186.
17. M. C. WEINBERG, *J. Amer. Ceram. Soc.* **74** (1991) 1905.
18. K. F. KELTON, *ibid.* **75** (1992) 2449.
19. A. K. CHEETAM, G. FEREY and T. LOISEAN, *Angew. Che. Ed.* **38** (1999) 3268.
20. Y. NAN, W. E. LEE and P. F. JAMES, *J. Amer. Ceram. Soc.* **75** (1992) 1641.
21. HSC Chemistry (Outokumpu Research Oy, Finland, 1993).
22. W. D. KINGERY, H. K. BOWEN and D. R. UHLMANN, "Introduction to Ceramics" (John Wiley & Sons, New York, London, 1976).
23. Z. QIAN, T. L. TOLT and A. R. COOPER, *J. Amer. Ceram. Soc.* **70** (1987) /1/49.
24. K. MATUSITA and S. SAKA, *Physics Chem. Glasses* **20** (1979) 81.
25. M. C. WEINBERG, *J. Non-Cryst. Solids* **127** (1991) 151.
26. K. F. KELTON, *Mater. Sci. Eng.* A **226–228** (1997) 142.
27. T. OZAWA, *Polymer* **12** (1971) 150.
28. J. W. CHRISTIAN, "The Theory of Transformations in Metals and Alloys" (Pergamon Press, Oxford, 1975).

Received 23 April
and accepted 25 November 2002